Original Scientific Paper https://doi.org/10.24867/GRID-2026-p19

Printing Possibility on Biopolymer Based Films

ABSTRACT

The growing demand for sustainable packaging and printed products has increased interest in biodegradable polymeric materials as environmentally friendly alternatives to conventional plastics. However, their printability and color reproduction characteristics remain insufficiently investigated. This study evaluates the suitability of biodegradable polymer films based on poly (lactic acid) (PLA) and its blends with poly (butylene succinate) (PBS), poly (hydroxybutyrate) (PHB), and poly (hydroxybutyrate-co-valerate) (PHBV) for UV inkjet printing applications. Biopolymer films were produced by flat-die extrusion under controlled processing conditions. The printed samples were obtained using a UV inkjet printing system under standardized printing parameters. Print quality was assessed through optical density and CIELAB color measurements using a spectrophotometer, while the chemical structure of the prepared blends was examined by FTIR spectroscopy to verify the absence of chemical reactions during processing. The obtained results indicate that all investigated biopolymer blends provide high optical density values with only minor variations among formulations. Although differences in lightness (L) were observed between individual blends, chromatic coordinates (a* and b*) remained relatively stable, demonstrating consistent color reproduction across the tested materials. FTIR analysis confirmed that no new chemical bonds were formed during extrusion, indicating that the prepared materials represent physical polymer blends. The findings demonstrate that PLA-based biodegradable films and their blends exhibit promising printability for UV inkjet technology while maintaining their chemical integrity after processing. These results contribute to the development of sustainable printed products and provide a basis for further optimization of biodegradable substrates intended for graphic and packaging applications.*

Ivana Jurič [1]
Aleksandra Nešić [2]
Branka Pilić [2]
Nemanja Kašiković [1]
Magdolna Pál [1]
Živko Pavlović [1]

[1] University of Novi Sad, Faculty of Technical Sciences, Department of Graphic Engineering and Design, University of Novi Sad, Novi Sad, Serbia
[2] University of Novi Sad, Faculty of Technology, Novi Sad, Serbia

KEY WORDS
UV inkjet printing, biopolymer films, PLA blends, color reproduction, print quality, FTIR analysis, sustainable packaging

1. Introduction

The excessive use and inadequate disposal of petroleum-derived plastics have led to significant environmental pollution and to the accumulation of plastic waste in terrestrial and aquatic ecosystems (Taib et al., 2024). Conventional polymers such as low-density polyethylene (LDPE) are widely used in flexible packaging because of their low cost and ease of processing; however, they are poorly recycled due to their flexible nature and low residual economic value (Taib et al., 2024). This situation has driven substantial research effort toward biodegradable and bio-based alternatives for packaging applications (Kricheldorf, 2005). Poly(lactic acid) (PLA) has emerged as one of the most commercially attractive biopolymers for sustainable packaging, offering renewability from agricultural feedstocks, good mechanical properties, transparency and biocompatibility (Kricheldorf, 2005). Nevertheless, PLA exhibits limitations that restrict its stand-alone use in flexible packaging, including inherent brittleness, low ductility, limited thermal endurance and weak moisture barrier properties (Kricheldorf, 2005; Ali et al., 2023). To overcome these limitations, PLA is frequently blended with other biodegradable polyesters,

in particular poly(butylene succinate) (PBS), poly(hydroxybutyrate) (PHB) and poly(hydroxybutyrate-co-hydroxyvalerate) (PHBV), the latter two being important members of the polyhydroxyalkanoate family (Chuakhao et al., 2024; Patel et al., 2022; Tubio et al., 2023).
PBS is a semicrystalline biodegradable polyester that, when blended with PLA, improves ductility and processability while preserving biodegradability and compostability (Chuakhao et al., 2024). PHB, the principal member of the polyhydroxyalkanoates, exhibits exceptionally high crystallinity (up to 70–75 wt%), which results in a high elastic modulus and tensile strength comparable to conventional petrochemical polymers such as polystyrene (Patel et al., 2022). Blending PLA with PHB improves overall crystallinity and the barrier properties essential for food packaging (Pate Patel).
PHBV, a copolymer of hydroxybutyrate and hydroxyvalerate, combines the rigidity of PHB with enhanced flexibility and elasticity (Tubio et al., 2023) PHBV/PLA blends have been reported to yield films with improved mechanical characteristics and increased hydrophilicity compared with neat PHBV (Tubio et al., 2023).

Printability is a critical requirement for packaging materials, yet the surface properties that govern ink anchorage on biopolymer blends remain insufficiently characterized. Surface energy, wettability, roughness and topography together determine ink–substrate interactions and, ultimately, print quality (Mahović Poljaček, Tomašegović & Priselac, 2026). The adhesion of printing inks depends on the reciprocal interaction of the polar and dispersive components of the surface free energy of the film and of the ink; greater similarity between these components results in improved wetting and adhesion (Mahović). Because biopolymer blends generally exhibit phase-separated morphologies, with surface characteristics inherited from each component, their printing behavior may differ appreciably from that of single-polymer systems (Mahović Poljaček, Tomašegović & Priselac, 2026).

A growing body of work has specifically addressed the printability of PLA and its blends. Early flexographic trials on neat PLA film showed that it could reproduce solid tones and half-tone dots to a standard comparable with conventional PET and OPP substrates, although its inherently low surface energy required careful matching of ink formulation, anilox volume and plate screen ruling (Rong & Keif, 2007; Jacobson et al., 2009). Because untreated PLA surfaces are non-polar and offer limited wettability, several studies ; have turned to plasma activation as a pretreatment: oxygen and argon plasma applied to PLA film raised its surface free energy sufficiently to improve flexographic solid-tone density and dot quality (Izdebska-Podsiadły, 2021), while low-pressure plasma applied to PLA/PHB blends plasticized with acetyl tributyl citrate increased surface energy in a way that depended jointly on plasma power, exposure time and blend composition (Omaníková et al., 2020). Closer to the present study, a preliminary investigation of digital printing on biodegradable flexible packaging materials reported that the choice of biodegradable substrate measurably narrows the reproducible colour gamut relative to conventional films (Maňúrová, Preklet & Horváth, 2021). Taken together, these studies establish that PLA and simple PLA blends can be printed to an acceptable standard, but each is limited either to a single polymer, to flexographic rather than inkjet technology, to the effect of an additional surface treatment, or to the reproducible colour gamut rather than the optical density and CIELAB coordinates of a standardized full-tone patch. None examines UV inkjet printing on PLA blended systematically with PBS, PHB and PHBV across a composition range, which is the specific gap addressed here.

UV inkjet technology offers clear advantages for packaging: it is essentially solvent-free, cures by rapid photopolymerisation, and has a reduced environmental footprint compared with conventional solvent-based processes (Kováčik et al., 2024). Modern UV inks are formulated to adhere to a wide range of polymer surfaces, which in principle enables printing on sustainable biopolymer substrates (Kováčik et al., 2024)). However, the compatibility and colour reproduction behavior of UV inks on PLA/PBS, PLA/PHB and PLA/PHBV blend films have not been systematically investigated. It is not known whether variation of the second blend component and its mass fraction — which changes crystallinity, phase morphology and surface topography of the film — translates into measurable differences in optical density or in reproduced colour. A further and largely unaddressed question is methodological: extruded biopolymer films frequently exhibit a pronounced machine-direction line structure and micro-relief, and it is unclear to what extent conventional spectrophotometric evaluation of such surfaces reports genuine colour differences rather than artefacts of measurement geometry.

The objectives of the present study were therefore fourfold: (i) to verify, by ATR-FTIR spectroscopy, that flat-die extrusion of PLA with PBS, PHB and PHBV yields physical blends rather than reactively compatibilized systems; (ii) to quantify the optical density and CIELAB coordinates of full-tone black UV inkjet prints on ten extruded biopolymer films; (iii) to evaluate, through total colour differences in both the CIE 1976 and CIEDE2000 metrics, whether the choice and concentration of the second blend component compromises the consistency of colour reproduction and the machine readability of printed graphic elements; and (iv) to assess the contribution of surface texture to the measured variability and to derive practical recommendations for the colorimetric quality control of printed biodegradable films.

2. Materials and methods

2.1. Materials

Poly(lactide) (PLA) INGEO 2003D (NatureWorks LLC, USA) was used as the main component in all blends. Poly(butylene succinate) (PBS) was supplied by NaturePlast (France). Poly(hydroxybutyrate) (PHB) and poly(hydroxybutyrate-co-hydroxyvalerate) (PHBV) were purchased from Helian Polymers (The Netherlands), grades ENMAT Y3000P and ENMAT Y1000P, respectively. All polymers were dried prior to extrusion in order to prevent hydrolytic degradation of the polyester chains during melt processing.

Prints were produced using the standard CMYK ink set of the press manufacturer. For colorimetric measurement, printed films were backed by a uniform white substrate (Options cool white, 220 g/m²; measured CIELAB values L* = 95.84 ± 0.16, a* = 1.94 ± 0.04, b* = −3.60 ± 0.09; mean of five measurements) so that the semi-transparent films were evaluated against a reproducible and standardized background.

2.2. Film preparation

Films were produced by flat-die extrusion on a custom-built single-screw extruder. Polymer pellets were dry-mixed in the required mass ratio immediately before processing and fed into the extruder hopper without prior compounding, so that blending occurred in the melt during a single extrusion pass. The extruded melt was drawn through a flat die and taken up by a calender. All samples were processed with the calender cooled, with the single exception of sample PLA16, which was produced without calender cooling in order to evaluate the influence of the cooling regime — and hence of the surface topography and degree of crystallinity of the film — on the subsequent print result. The sample designation used throughout this work combines the abbreviation of the second blend component with its nominal mass fraction in the blend: PHB10 denotes a film containing 90 wt% PLA and 10 wt% PHB, PHBV30 a film containing 70 wt% PLA and 30 wt% PHBV, and so forth. Samples PLA15 and PLA16 are neat PLA films and serve as the reference for all blends. The complete list of samples and the corresponding processing parameters is given in Table 1.

2.3. FTIR analysis

Fourier-transform infrared spectroscopy of the prepared films was performed on an IRAffinity-1S spectrometer equipped with an attenuated total reflectance (ATR) accessory (Shimadzu, Japan). Transmittance (T, %) was recorded over the range 400–4000 cm–1 at a spectral resolution of 4 cm–1, accumulating 40 scans per spectrum. Spectra of the neat components were recorded under identical conditions and used as references. The purpose of the analysis was to confirm that no reactive extrusion had taken place and that only physical blends were obtained, which is a prerequisite for interpreting the optical results in terms of blend morphology rather than of newly formed chemical species.

2.4. Printing

Printing was performed on an ArtisJet 3000U flat-bed UV inkjet printer. A dedicated test chart was designed for the study, containing full-tone patches of the process colours, tonal step wedges and QR code elements of graded module size. All samples were printed in a single production run using the standard machine settings in KCMY mode, without an opaque white underprint layer, so that the interaction between the ink and the bare biopolymer surface — rather than between the ink and an interme-

Table 1

List of investigated samples and flat-die extrusion processing parameters

Sample	T zone 1 (°C)	T zone 2 (°C)	T zone 3 (°C)	Screw speed (rpm)	Calender speed (m/min)
PLA15	165	170	175	90	2
PLA16 *	165	170	175	90	2
PHB10	160	165	170	50	1
PHB20	160	165	170	50	1
PHB30	165	170	175	100	2
PBS10	165	170	175	100	2
PBS20	165	170	175	100	2
PHBV10	165	170	175	100	2
PHBV20	165	170	175	100	2
PHBV30	165	170	175	100	2

* Processed without cooling the calender. Sample designation: the numerical suffix denotes the nominal mass fraction (wt%) of the second component in the PLA-based blend; PLA15 and PLA16 are neat PLA films

diate primer — determined the print result. Curing was performed by the integrated UV lamp assembly of the press under nominal settings. Printed films were conditioned for 24h at room temperature before measurement to allow complete dark cure and relaxation of the ink film.

2.5. Optical density and colorimetric measurement

Optical density (D) and CIELAB coordinates (L*, a*, b*) of the full-tone black patches were measured with a Techkon SpectroDens spectrodensitometer. The instrument was calibrated on absolute white before each measurement series. Measurements were carried out using the CIE standard illuminant D50 and the CIE 1931 2° standard observer. Five independent measurements were taken at different positions of each printed patch, giving fifty readings in total, and the results are reported as arithmetic mean ± standard deviation. Measuring at several positions was considered essential, because extruded biopolymer films may exhibit a pronounced micro-relief and machine-direction line structure that can locally modify the measurement geometry; as shown in Section 3.5, this precaution proved decisive for the interpretation of the results.

Surface appearance of the printed films was additionally inspected with a VT300 digital portable microscope. Machine readability of the printed QR codes was verified using two commercially available mobile devices with different camera systems and decoding libraries — an Apple iPhone 15 (iOS) and a Xiaomi Redmi Note 10 Pro (Android) — each code being tested on both devices under diffuse office illumination.

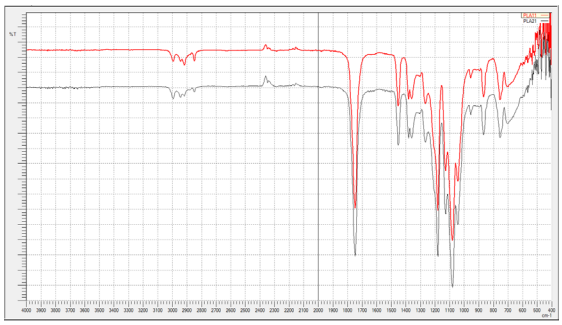
2.6. Evaluation of colour differences and statistical analysis

Total colour differences between printed samples were calculated according to the CIE 1976 colour difference formula. Because the CIE 1976 (ΔE76) metric is known to overstate lightness differences in dark colours, all pairwise differences were additionally recalculated in the CIEDE2000 metric (ΔE00), using the standard parametric weighting factors kL = kC = kH = 1. Chroma and hue angle were derived as $C^*ab = (a^{*2} + b^{*2})1/2$ and hab = arctan(b*/a*). In the interpretation of the results, the conventional perceptibility threshold of ΔE ≈ 1 for a trained observer under optimal viewing conditions and the acceptability threshold of ΔE ≈ 3 for commercial print reproduction were used as reference levels. The statistical significance of differences among the ten samples was assessed by one-way analysis of variance (ANOVA) applied separately to D, L*, a* and b*, followed by Welch's t-test for selected pairwise comparisons. The relationship between optical density and lightness was examined by Pearson correlation, both across sample means and across all fifty individual readings. A significance level of α = 0.05 was adopted throughout. All calculations were performed on the complete set of individual measurements rather than on pre-aggregated values.

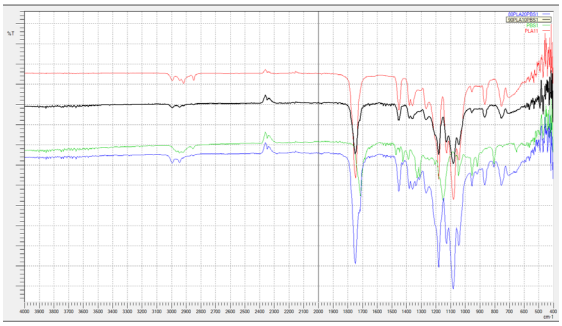
3. Results and discussion

3.1. FTIR analysis — confirmation of physical blending

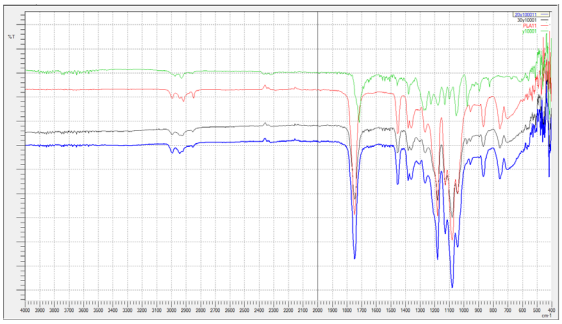
FTIR spectra of all samples showed no chemical reaction between PLA and other biopolymers in the blend, since no new peaks occurred in the spectra. Comparison of the FTIR spectra between pure components and blends is shown in Figure 1.



(a)

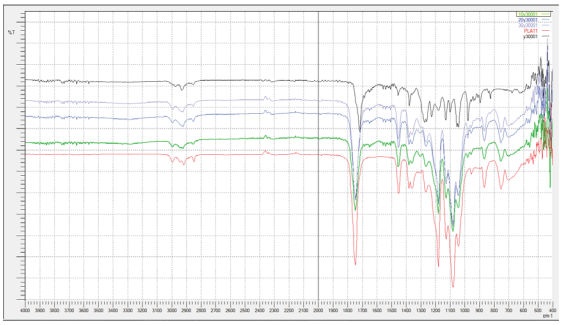


(b)



(c)

» **Figure 1 (part 1):** *FTIR Spectra of pure components and blends (a) PLA1-PLA2, (b) PBS-based series of samples, (c) PHBV-based series of samples and (d) PHB-based series of samples*



(d)

» **Figure 1 (part 2):** *FTIR Spectra of pure components and blends (a) PLA1-PLA2, (b) PBS-based series of samples, (c) PHBV-based series of samples and (d) PHB-based series of samples*

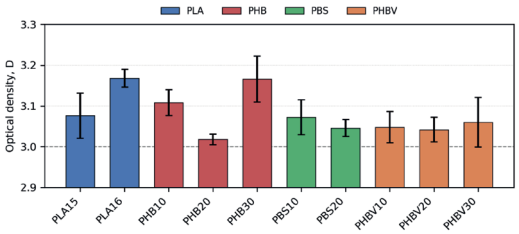
3.2. Optical density of the printed films

The measured optical density and CIELAB coodinates of the full-tone black UV inkjet prints are summarized in Table 2; the corresponding distributions are shown in Figures 2 and 3.

Optical density proved to be uniformly high on every substrate. All fifty individual readings fell between D = 3.00 and D = 3.20, and the sample means occupied the narrow interval 3.018–3.168 with a grand mean of 3.080. An optical density above 3.0 corresponds to transmission of less than 0.1% of the incident light through the printed layer, indicating excellent ink holdout and complete coverage on all ten films. Not a single measurement position on any formulation failed to reach this level.

Within this narrow band the differences between samples are nevertheless statistically significant (ANOVA: $F(9,40) = 8.16$; $p < 0.001$). The highest densities were recorded on PLA16 (3.168 ± 0.022) and PHB30 (3.166 ± 0.056) and the lowest on PHB20 (3.018 ± 0.013). The total spread of 0.15 density units is small in absolute terms, but it is not negligible by the standards of process control in commercial printing, where full-tone density tolerances of ±0.05–0.10 are typical. Substrate selection therefore has a measurable, if modest, influence on solid density and should be considered when a common density target is applied across several film types.

It is notable that the ranking of densities does not follow the mass fraction of the second component in any of the three blend families. Within the PHB series the density falls from 3.108 at 10 wt% to 3.018 at 20 wt% and then rises to 3.166 at 30 wt%; within the PHBV series it varies by only 0.018 units across the whole concentration range. Composition alone therefore does not explain the observed behavior, which points instead to the processing conditions and the resulting surface state of the film — an interpretation developed further in Sections 3.3 and 3.5.



» **Figure 2:** *Optical density (D, mean ± SD, n = 5) of full-tone black UV inkjet prints on the investigated biopolymer films. The dashed line marks D = 3.0*

3.3. Lightness of the printed films

Lightness is by far the most variable of the measured quantities. The sample means span L* = 13.32–24.96, a range of 11.65 units, and the individual readings extend from 12.90 to 26.82. The differences between formulations are highly significant (ANOVA: $F(9,40) = 14.35$; $p < 0.001$). PHB30 produced the visually deepest black of the study (13.32 ± 0.66), followed by PLA16 (15.68 ± 0.44), while PBS20 gave by far the lightest result

Table 2

Optical density and CIELAB coordinates of full-tone black UV inkjet prints on the investigated biopolymer films (mean ± SD, n = 5)

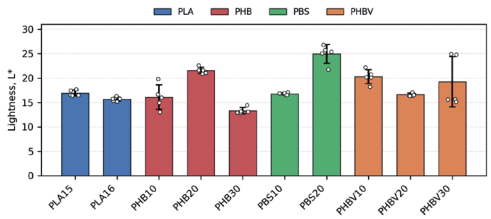
Sample	D	L*	a*	b*
PLA15	3.076 ± 0.055	16.93 ± 0.60	1.65 ± 0.15	−0.47 ± 0.26
PLA16	3.168 ± 0.022	15.68 ± 0.44	1.62 ± 0.10	−0.71 ± 0.14
PHB10	3.108 ± 0.032	16.11 ± 2.50	1.71 ± 0.10	−0.33 ± 0.23
PHB20	3.018 ± 0.013	21.57 ± 0.65	1.97 ± 0.10	−0.32 ± 0.18
PHB30	3.166 ± 0.056	13.32 ± 0.66	1.80 ± 0.47	−0.67 ± 0.61
PBS10	3.072 ± 0.043	16.79 ± 0.25	1.63 ± 0.21	−0.71 ± 0.14
PBS20	3.046 ± 0.021	24.96 ± 1.91	1.84 ± 0.19	−0.77 ± 0.09
PHBV10	3.048 ± 0.038	20.30 ± 1.42	1.82 ± 0.06	−0.53 ± 0.06
PHBV20	3.042 ± 0.030	16.61 ± 0.30	1.76 ± 0.19	−0.49 ± 0.30
PHBV30	3.060 ± 0.061	19.23 ± 5.15	1.75 ± 0.17	−0.58 ± 0.22

(24.96 ± 1.91), with PHB20 (21.57 ± 0.65) and PHBV10 (20.30 ± 1.42) also at the light end of the scale.

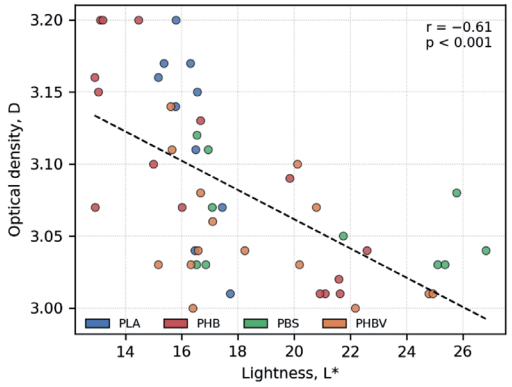
Critically, lightness does not vary monotonically with the concentration of the second blend component in any of the three families. In the PHB series L* rises from 16.11 at 10 wt% to 21.57 at 20 wt% and then falls sharply to 13.32 at 30 wt%, a non-monotonic excursion of more than eight units. In the PHBV series the sequence is 20.30 → 16.61 → 19.23, again with the intermediate concentration as the extreme value. Only the PBS series shows a simple increase, from 16.79 to 24.96. If the mass fraction of the minor phase were the controlling variable, a consistent and preferably monotonic trend would be expected in each family; its absence indicates that composition is not the dominant factor.

Two other observations support this conclusion. First, the two neat PLA films differ significantly from one another (L* = 16.93 ± 0.60 versus 15.68 ± 0.44; Welch's t = 3.74; p = 0.007), even though they are chemically identical and were extruded at the same temperatures and screw speed. The only difference between them is that PLA16 was processed without calender cooling. A change in the cooling regime, which alters the degree of crystallinity, the surface gloss and the micro-topography of the film without altering its chemistry, is therefore sufficient to shift measured lightness by more than one unit and to raise optical density by 0.09. Second, the two samples extruded at the reduced calender speed of 1 m/min (PHB10 and PHB20) behave very differently from one another, which again cannot be attributed to composition alone.

Lightness and optical density are strongly and inversely correlated, as physical consistency requires: r = −0.73 (p = 0.016) across the ten sample means and r = −0.61 (p < 0.001) across all fifty individual readings (Figure 4). Darker prints return higher density readings, and the two quantities respond to the same underlying property of the printed surface. This internal consistency provides useful validation of the measurement series, but it also means that the two parameters should not be treated as independent indicators of print quality.



» **Figure 3:** *Lightness (L*, mean ± SD, n = 5) of full-tone black UV inkjet prints on the investigated biopolymer films. Open circles show the five individual measurement positions per sample; note the two clearly separated populations of readings for PHBV30 and the wide spread for PHB10*



» **Figure 4:** *Relationship between lightness and optical density for all fifty individual measurements. The dashed line is the least-squares fit*

3.4. Chromatic coordinates

In sharp contrast to lightness, the chromatic coordinates are statistically indistinguishable across the entire material set. One-way ANOVA returns no significant effect of formulation either for a* (F(9,40) = 1.42; p = 0.21) or for b* (F(9,40) = 1.81; p = 0.10). The sample means are confined to a* = 1.62–1.97 and b* = −0.77 to −0.32, corresponding to chroma values of only C*ab = 1.71–2.00 and hue angles clustered between 336° and 351°. Every substrate therefore reproduces the full-tone black as an almost achromatic colour with a very slight warm-red cast and a marginal blue bias.

This is the central positive finding of the study for print production. The chemistry of the second blend component and its concentration do not measurably affect the hue or the saturation of the reproduced black. Where a difference appears at all, it is a difference in how light or dark the print is, not in what colour it is. Since colour management systems compensate for lightness far more readily than for hue shifts — a lightness offset can be corrected by a single adjustment of the tone reproduction curve, whereas a hue shift requires re-profiling — this behavior is considerably more favorable than the opposite pattern would be.

Nominally, the PBS-based films display the most negative b* values of the set (−0.71 and −0.77) and the PHB-based films at 10 and 20 wt% the least negative (−0.33 and −0.32), which would correspond to a marginally cooler black on PBS and a marginally warmer one on PHB. However, the within-sample standard deviations of b* are of the same order as these differences, reaching 0.61 for PHB30 and 0.30 for PHBV20, and the effect does not survive the analysis of variance. It should therefore be regarded as a tendency worth confirming in a larger series rather than as an established difference.

3.5. Surface texture and the reliability of the colorimetric data

The within-sample variability differs by more than an order of magnitude between formulations and deserves attention. The standard deviation of L* ranges from 0.25 for PBS10 and 0.30 for PHBV20 — values close to the repeatability of the instrument — to 1.91 for PBS20, 2.50 for PHB10 and 5.15 for PHBV30. Expressed as a coefficient of variation, the spread reaches 26.8% for PHBV30 and 15.5% for PHB10, against 1.5% for PBS10.

The pattern of the individual readings is more revealing than the summary statistics. For PHBV30 the five measurement positions returned L* values of 15.16, 15.61, 15.65, 24.79 and 24.93: two tightly grouped populations separated by more than nine lightness units, with no intermediate values. The arithmetic mean of 19.23 corresponds to no physical location on the sample, and the median of 15.65 differs from it by 3.58 units. A comparable, though less extreme, dispersion is seen for PHB10, where the readings range from 13.03 to 19.84. Such bimodality cannot arise from the colour of a homogeneously printed ink layer; it indicates that the measuring aperture encountered two distinct surface states on the same specimen.

Microscopic inspection of these films showed pronounced machine-direction lines and a distinct micro-relief. Surface structure of this kind alters the local measurement geometry: depending on the orientation of the relief relative to the measuring beam, the aperture may collect an increased specular component or, conversely, fall within a locally shaded region. The instrument registers both cases as a change in lightness. Part of the apparent colour difference between textured samples is therefore of instrumental rather than colorimetric origin, whereas the human visual system, which integrates over a larger field and compensates for surface gradients, does not perceive a comparable difference. This mechanism also explains why the samples with the smoothest measured behavior (PBS10, PHBV20) are those with the lowest dispersion, and why formulation alone fails to account for the lightness ranking discussed in Section 3.3.

Three practical consequences follow. Spectrophotometric data on textured biodegradable films should be acquired at several positions sufficient to reveal multimodality — five is a workable minimum, but more are advisable for visibly structured surfaces — and the individual readings, not only the mean, should be inspected. Where the distribution is clearly bimodal, the median or a mode-resolved analysis is more informative than the arithmetic mean. Finally, instrumental results on such substrates should be corroborated by visual assessment before a batch is rejected on colorimetric grounds.

3.6. Total colour differences

The complete matrix of total colour differences calculated according to Eq. (1) is given in Table 3 and visualized in Figure 5; the corresponding CIEDE2000 values are given in Table 4.

The largest difference in the set, ΔE*ab = 11.65, separates PHB30 from PBS20 — the darkest and the lightest formulation. Nine of the forty-five pairwise comparisons exceed 5 units and would be plainly visible in a side-by-side presentation. At the other extreme, the closest pairs are PLA15–PBS10 (0.28), PBS10–PHBV20 (0.31) and PLA15–PHBV20 (0.34), all well below the perceptibility threshold, showing that films of quite different chemical composition can be colorimetrically interchangeable.

Unlike in a conventional substrate series, the differences do not organize themselves by polymer family. Within the PHB series the three concentrations differ by 2.81 to 8.26 units, and the two PBS films differ by 8.18 units, whereas members of different families may be nearly identical. In every case the difference is dominated by ΔL*: the chromatic contributions Δa* and Δb* never exceed 0.5 units and typically contribute less than 2% to the value of Eq. (1). Expressed differently, Table 3 is essentially a map of lightness differences, and in view

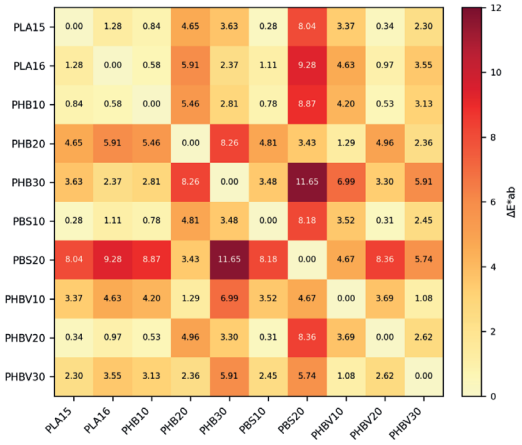
Table 3

Matrix of total colour differences ΔE*ab (CIE 1976) between all pairs of printed biopolymer films

	PLA15	PLA16	PHB10	PHB20	PHB30	PBS10	PBS20	PHBV10	PHBV20	PHBV30
PLA15	0.00	1.28	0.84	4.65	3.63	0.28	8.04	3.37	0.34	2.30
PLA16	1.28	0.00	0.58	5.91	2.37	1.11	9.28	4.63	0.97	3.55
PHB10	0.84	0.58	0.00	5.46	2.81	0.78	8.87	4.20	0.53	3.13
PHB20	4.65	5.91	5.46	0.00	8.26	4.81	3.43	1.29	4.96	2.36
PHB30	3.63	2.37	2.81	8.26	0.00	3.48	11.65	6.99	3.30	5.91
PBS10	0.28	1.11	0.78	4.81	3.48	0.00	8.18	3.52	0.31	2.45
PBS20	8.04	9.28	8.87	3.43	11.65	8.18	0.00	4.67	8.36	5.74
PHBV10	3.37	4.63	4.20	1.29	6.99	3.52	4.67	0.00	3.69	1.08
PHBV20	0.34	0.97	0.53	4.96	3.30	0.31	8.36	3.69	0.00	2.62
PHBV30	2.30	3.55	3.13	2.36	5.91	2.45	5.74	1.08	2.62	0.00

of Section 3.5 a substantial part of those differences reflects surface texture rather than the print itself.

This interpretation is reinforced by the CIEDE2000 recalculation. The CIE 1976 metric is known to exaggerate lightness differences in dark colours, where the lightness weighting function of CIEDE2000 takes values around 1.5. Recalculating in ΔE00 reduces the maximum difference from 11.65 to 7.99, the PHB20–PHB30 difference from 8.26 to 5.57, and the PBS10–PBS20 difference from 8.18 to 5.72 — a systematic reduction of roughly 30% for the lightness-driven pairs, while the already small chromatic differences are essentially unchanged (PLA15–PBS10: 0.28 versus 0.25). The choice of colour difference metric therefore has a material effect on the conclusions, and reporting ΔE*ab alone overstates the magnitude of the substrate effect for dark tones.



» **Figure 5:** *Heat map of the total colour differences ΔE*ab between all pairs of printed biopolymer films.*

3.7. Print–substrate contrast and functional readability

For printed packaging the decisive criterion is frequently not the absolute colour of the ink but the contrast it forms with the unprinted substrate, because this contrast governs the legibility of text and the machine readability of coded graphic elements. Measured against the white backing (L* = 95.84, a* = 1.94, b* = −3.60), the full-tone black prints yield total colour differences of ΔE*ab = 70.9–82.6. The spread of some twelve units across the material set, though it mirrors the lightness differences discussed above, is negligible relative to the absolute contrast achieved: the weakest-contrast substrate, PBS20, still delivers ΔE*ab = 70.9.

Consistent with this, all printed QR codes were decoded successfully on every substrate, using both test devices and both operating systems, and across the full range of module sizes present on the test chart. Neither the choice of the second blend component nor its mass fraction, nor the calender cooling regime, impaired the machine readability of the printed elements. The uniformly high optical density (every reading above D = 3.0) provides the luminance contrast required by the decoding algorithms with a substantial margin, and differences of ten lightness units in a colour whose L* is below 25 are immaterial at this scale.

Taken together with the FTIR results, these findings show that the functional performance of the print is decoupled from the formulation of the film within the composition range studied. Blend composition can therefore be selected based on mechanical, thermal and barrier requirements, or of cost and end-of-life considerations, without a penalty in functional printability.

Table 4

Matrix of total colour differences ΔE00 between all pairs of printed biopolymer films

	PLA15	PLA16	PHB10	PHB20	PHB30	PBS10	PBS20	PHBV10	PHBV20	PHBV30
PLA15	0.00	0.87	0.57	3.21	2.40	0.25	5.63	2.31	0.27	1.57
PLA16	0.87	0.00	0.48	4.06	1.57	0.74	6.45	3.15	0.68	2.40
PHB10	0.57	0.48	0.00	3.75	1.86	0.59	6.18	2.86	0.37	2.12
PHB20	3.21	4.06	3.75	0.00	5.57	3.33	2.48	0.93	3.41	1.67
PHB30	2.40	1.57	1.86	5.57	0.00	2.30	7.99	4.68	2.17	3.94
PBS10	0.25	0.74	0.59	3.33	2.30	0.00	5.72	2.41	0.30	1.67
PBS20	5.63	6.45	6.18	2.48	7.99	5.72	0.00	3.33	5.84	4.06
PHBV10	2.31	3.15	2.86	0.93	4.68	2.41	3.33	0.00	2.51	0.75
PHBV20	0.27	0.68	0.37	3.41	2.17	0.30	5.84	2.51	0.00	1.77
PHBV30	1.57	2.40	2.12	1.67	3.94	1.67	4.06	0.75	1.77	0.00

3.8. Practical implications and limitations

Several recommendations follow production practice. Where the deepest possible black is required — for high-contrast codes or fine reversed-out typography — PHB30 and the uncooled PLA16 are the preferred substrates, combining the lowest lightness with the highest optical density. Where colour consistency across several substrates is the priority, PLA15, PBS10 and PHBV20 form a group that is mutually interchangeable within the perceptibility threshold and can be run to a single colour standard. Where a film with visible surface structure must be used, the quality-control protocol should be adapted as described in Section 3.5 rather than the material being rejected based on a single measurement. In all cases, the chromatic dimensions require no attention: hue and saturation are stable across the entire material set.

Several limitations should be acknowledged. The study evaluated a single UV inkjet system under standard settings and without an opaque white underprint; other ink chemistries, curing configurations or the introduction of a white base layer would be expected to shift the absolute values, although the relative behavior of the substrates should be preserved. Only full-tone black was analyzed in depth, so tonal reproduction, dot gain and the behavior of the chromatic process inks remain to be characterized. Five measurement positions per sample proved sufficient to reveal multimodality but are too few to characterize the underlying distributions quantitatively; a denser sampling grid, ideally combined with profilometric mapping of the same positions, is the obvious next step and would allow the contribution of surface relief to be separated from that of the print. Surface free energy, roughness and ink adhesion were not measured, which limits the mechanistic interpretation of the differences between formulations. Finally, the prints were evaluated shortly after production, so the long-term stability of the ink film on biodegradable substrates — including light fastness, mechanical resistance and behavior during composting — was outside the scope of this work.

4. Conclusions

This study evaluated the UV inkjet printability of ten biodegradable films produced by flat-die extrusion: neat PLA processed with and without calender cooling, and PLA blends containing 10–30 wt% of PHB, PHBV or PBS. The following conclusions can be drawn.

FTIR spectroscopy confirmed that single-pass flat-die extrusion produced physical blends only. No new absorption bands appeared, and no bands of the neat components disappeared, so the optical behavior of the films reflects their phase morphology and surface topography rather than any newly formed chemical structure.

All ten substrates delivered high optical density of the full-tone black print. Every one of the fifty individual readings exceeded D = 3.00, and the sample means occupied the interval 3.018–3.168, indicating excellent ink holdout on all formulations.

Colour reproduction was consistent in the chromatic dimensions. Neither a* ($p = 0.21$) nor b* ($p = 0.10$) differed significantly between formulations; all prints remained confined to a near-neutral region with C*ab = 1.71–2.00 and hue angles between 336° and 351°. The identity and concentration of the second blend component do not affect the hue or saturation of the reproduced black.

Lightness, by contrast, varied significantly between formulations (L* = 13.32–24.96; $p < 0.001$) and was inversely correlated with optical density ($r = -0.61$ across all readings; $p < 0.001$). The variation was not monotonic with the concentration of the second component, and the two chemically identical neat PLA films differed significantly from one another, which shows that processing conditions — in particular the calender cooling regime — and the resulting surface state, rather than blend composition alone, govern this parameter.

Surface texture was shown to contribute substantially to the measured variability. Within-sample standard deviations of L* ranged from 0.25 to 5.15, and PHBV30 returned two clearly separated populations of readings differing by more than nine lightness units. Spectrophotometric evaluation of structured biodegradable films must therefore be based on multiple measurement positions, on inspection of the individual readings rather than the mean alone, and on corroboration by visual assessment.

Total colour differences reached ΔE*ab = 11.65 at most and were dominated almost entirely by lightness, the chromatic contributions never exceeding 0.5 units. Recalculation in the CIEDE2000 metric reduced the lightness-driven differences by approximately 30% (maximum ΔE00 = 7.99), confirming that the CIE 1976 formula overstates the substrate effect for dark tones and that ΔE00 should be preferred when evaluating black prints on such materials.

Print–substrate contrast reached ΔE*ab = 70.9–82.6 on every film, and all printed QR codes were decoded successfully on two independent mobile platforms, confirming that functional graphic elements are reproduced reliably on all the biopolymer films investigated.

Overall, PLA-based biodegradable films and their blends with PBS, PHB and PHBV exhibit promising printability for UV inkjet technology while retaining their chemical integrity after processing. Blend composition can be optimized for mechanical, barrier and end-of-life performance without compromising the chromatic consistency

of the print or the functionality of machine-readable elements, provided that the lightness of the reproduction and the surface texture of the film are controlled at the process level. These results contribute to the development of sustainable printed products and provide a basis for further optimization of biodegradable substrates intended for graphic and packaging applications.

5. Acknowledgments

This research has been supported by the Ministry of Science, Technological Development and Innovation (Contract No. 451-03-34/2026-03/200156) and the Faculty of Technical Sciences, University of Novi Sad through project “Scientific and Artistic Research Work of Researchers in Teaching and Associate Positions at the Faculty of Technical Sciences, University of Novi Sad 2026” (No. 01-3609/1).

6. References

Ali, W., Ali, H., Gillani, S., Zinck, P. and Souissi, S. (2023) 'Polylactic acid synthesis, biodegradability, conversion to microplastics and toxicity: A review', *Environmental Chemistry Letters*, 21(3), pp. 1761–1786. DOI: 10.1007/s10311-023-01564-8

Chuakhao, S., Rodríguez, J.T., Lapnonkawow, S., Kannan, G., Müller, A.J. and Suttiruengwong, S. (2024) 'Formulating PBS/PLA/PBAT blends for biodegradable, compostable packaging: The crucial roles of PBS content and reactive extrusion', *Polymer Testing*, 132, 108383. DOI: 10.1016/j.polymertesting.2024.108383

Izdebska-Podsiadły, J. (2021) 'Effect of plasma surface modification on print quality of biodegradable PLA films', *Applied Sciences*, 11(17), 8245. DOI: 10.3390/app11178245

Jacobson, J., Keif, M., Rong, X., Singh, J. and Vorst, K. (2009) 'Flexography printing performance of PLA film', *Journal of Applied Packaging Research*, 3(2), pp. 91–104.

Kováčik, D., Fleischer, M., Tučeková, Z., Baťková, E. and Kolářová, T. (2024) 'Plasma treatment of large-area polymer substrates for the enhanced adhesion of UV–digital printing', *Nanomaterials*, 14(5), 426. DOI: 10.3390/nano14050426

Kricheldorf, H.R. (2005) 'Polylactic acid'. In: Handbook of Polymer Synthesis. Volume 2. New York, NY: Marcel Dekker, pp. 347–370.

Mahović Poljaček, S., Tomašegović, T. and Priselac, D. (2026) 'Toward sustainable printed packaging: Surface properties and ink adhesion behavior of PLA/PCL/nanosilica biopolymer blends', *Polymers*, 18(3), 422. DOI: 10.3390/polym18030422

Maňúrová, K., Preklet, E. and Horváth, C. (2021) 'Investigation of printable color gamut in digital printing on biodegradable flexible packaging materials'. In: *Proceedings of the 2nd International Conference on Circular Packaging, 9–10 September 2021, Slovenj Gradec, Slovenia*.

Omaníková, L., Bočkaj, J., Černák, M., Plavec, R., Feranc, J. and Jurkovič, P. (2020) 'Influence of composition and plasma power on properties of film from biodegradable polymer blends', *Polymers*, 12(7), 1592. DOI: 10.3390/polym12071592

Patel, M.K., Zaccone, M., De Brauwer, L., Nair, R., Monti, M., Martinez-Nogues, V., Frache, A. and Oksman, K. (2022) 'Improvement of poly(lactic acid)–poly(hydroxy butyrate) blend properties for use in food packaging: Processing, structure relationships', *Polymers*, 14(23), 5104. DOI: 10.3390/polym14235104

Rong, X. and Keif, M. (2007) 'A study of PLA printability with flexography'. In: *TAGA Proceedings, 2007 Technical Association of the Graphic Arts Annual Technical Conference*, pp. 605–613.

Taib, S.M., Taib, N.M., Rahmat, A.R. and Adam, N.M. (2024) 'A review on bio-based polymer polylactic acid potential on sustainable food packaging', *Food Science and Biotechnology*, 33(2), pp. 307–328. DOI: 10.1007/s10068-024-01543-x

Tubio, C.R., Valle, X., Carvalho, E., Moreira, J., Costa, P., Correia, D.M. and Lanceros-Mendez, S. (2023) 'Poly(3-hydroxybutyrate-co-3-hydroxyvalerate) blends with poly(caprolactone) and poly(-lactic acid): A comparative study', *Polymers*, 15(23), 4566. DOI: 10.3390/polym15234566



© 2026 Authors. Published by the University of Novi Sad, Faculty of Technical Sciences, Department of Graphic Engineering and Design. This article is an open access article distributed under the terms and conditions of the Creative Commons Attribution license 4.0 Serbia (http://creativecommons.org/licenses/by/4.0/rs/).